

Microstructural and electrical characterizations of transparent Er-doped ZnO nano thin films prepared by sol–gel process

E. Asikuzun^{1,3,5} · O. Ozturk^{2,3} · L. Arda⁴ · C. Terzioglu⁵

Received: 21 April 2017 / Accepted: 2 June 2017 / Published online: 28 June 2017
© Springer Science+Business Media, LLC 2017

Abstract In this study, rare earth element (Er) doped ZnO nano thin films which have dual structure of $(\text{Zn}_{1-x}\text{Er}_x)\text{O}$ ($x=0.0, 0.01, 0.02, 0.03, 0.04$ and 0.05) are prepared by using sol–gel method. The microstructure and electrical properties of prepared nano thin films are investigated. Nano thin films are coated on the glass substrate by using the dip coating method. The films are annealed at 600°C for 30 min. The X-ray diffractometer (XRD), scanning electron microscopy and atomic force microscopy are used to determine the structural properties such as crystal structures, grain sizes, surface morphology; Hall effect measurements system is used to investigate the electrical properties of materials. XRD results showed that all Er doped nano thin films have a hexagonal structure and (002) orientation. Surface morphologies of ZnErO thin films are denser and more uniform than the undoped ZnO thin film. According to the Hall effect measurements, the resistivity of the films decreased with increasing Er concentration from 0 to 4% and then slightly increased at 5%Er.

1 Introduction

Transition metal and rare earth element doped ZnOs are called diluted magnetic semiconductors (DMS). DMS are ferromagnetic semiconductor materials that have the formula of $\text{Zn}_{1-x}\text{B}_x\text{O}$ (B; transition metal = Co, Mn, Cr, Fe, Cu, Ni, Al, Mg etc.) or $\text{Zn}_{1-x}\text{R}_x\text{O}$ (R; rare earth element = La, Y, Er, Cd, Yb, Ce etc.) and crystallize in wurtzite structure. Due to their different structural, electrical, magnetic and optical properties, ZnO and ZnO doped semiconductors have potential to be used in many different areas [1–10], such as giant magnetic resistance (GMR), tunnel magnetic resistance (TMR), spin-based light-emitting diodes, sensor and transistor devices that are promising especially in spintronics because of the controllability of electron spin with magnetic field.

Sol–gel process technique can be utilized for development of new nano-scale materials with room-temperature ferromagnetic properties at low cost. The development of these materials for electronics industry and the spintronics applications, in particular, will be important in terms of technological applications. There are many studies on the structural and electrical properties of DMS in the literature [11–14] but there are still continued problems. For example, formed residual stress and dislocation are reduced the performance of optoelectronic devices. In addition, determination of mechanical properties of these materials is worth for examination [15, 16].

In this study, we have investigated semiconductor thin films, namely Er doped ZnO. Structural properties such as lattice structure, surface morphology, grain size distribution of the prepared samples were characterized by Bruker D8 Advance X-ray powder diffractometer (XRD), Bruker model atomic force microscopy (AFM) and Quanta FEG 250 scanning electron microscopy (SEM). Electrical

✉ E. Asikuzun
easikuzun@kastamonu.edu.tr

¹ Department of Materials Science and Nanotechnology Engineering, Faculty of Engineering and Architecture, Kastamonu University, 37100 Kastamonu, Turkey

² Department of Physics, Faculty of Arts and Sciences, Kastamonu University, 37100 Kastamonu, Turkey

³ Research and Application Center, Kastamonu University, 37100 Kastamonu, Turkey

⁴ Department of Mechatronics Engineering, Faculty of Engineering and Natural Sciences, Bahcesehir University, 34349, Besiktas, Istanbul, Turkey

⁵ Department of Physics, Faculty of Arts and Sciences, Abant Izzet Baysal University, 14280 Bolu, Turkey

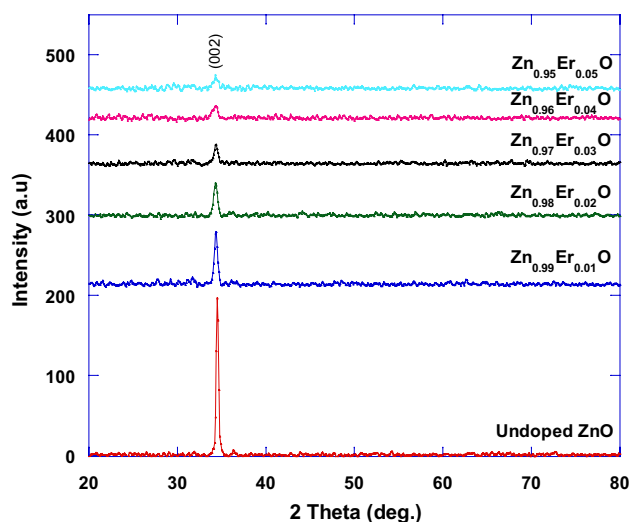


Fig. 2 XRD patterns of undoped ZnO and Er doped ZnO (with $x=0.0–0.5$) thin films

Table 2 Values of lattice parameter c , FWHM, grain size and average transmittance of undoped ZnO and Er doped ZnO thin films

Samples	c (002)	FWHM (deg.)	Grain size (nm)	Average transmittance (%)
Undoped ZnO	5.18	0.256	31.73	81.12
Zn _{0.99} Er _{0.01} O	5.21	0.444	18.32	89.15
Zn _{0.98} Er _{0.02} O	5.22	0.477	17.05	87.56
Zn _{0.97} Er _{0.03} O	5.22	0.506	16.07	84.93
Zn _{0.96} Er _{0.04} O	5.23	0.466	17.47	86.62
Zn _{0.95} Er _{0.05} O	5.23	0.498	16.32	87.14

peak intensity decreases with increasing Er doping. The increasing of Er concentration leads to deterioration of the ZnO crystal structure which is associated with the formation of the amorphous structure.

The FWHM value of the (002) peak is larger in the doped films than that in the undoped ZnO film (Table 2). These results show that the undoped ZnO films have higher crystallinity than doped ZnO nano thin film. The average grain size of undoped and Er doped ZnO nano thin films are calculated by using Scherer formula [21]. As can be seen from Table 2, particle size of nano thin films decreases from 31.73 to 16.32 nm with increasing the Er doping. Er doped ZnO nano thin films have smaller grain size than the undoped ZnO nano thin film. This size difference may be due to differences between ionic radius of doping element and zinc. These results are supported with our SEM analyses presented below.

3.1.2 SEM measurements

SEM images of undoped and Er doped ZnO films are shown in Fig. 3. The grain size of the undoped and Zn₉₅Er₀₅O films are 31.73 and 16.32 nm, respectively. Grain size is found to decrease with increasing Er doping [22] as observed from SEM pictures which are also supported by XRD data (Table 2). Surface morphology of doped thin films is denser than the undoped ZnO thin film.

3.1.3 AFM measurements

2D and 3D views of the surface morphology of Er doped ZnO-based semiconductor thin films are given in Fig. 4 (20×20 μm). As can be seen from the AFM images, surface morphology of thin films changes with an observed decrease in surface roughness with increasing Er doping. In our previous study [22], we have reported a sharp absorption in optical transmission measurements at wavelength range 360–400 nm (Fig. 5) for the same material system ZnO. The average optical transmittance is about 81% in the visible region (Table 2) for the undoped sample. Doping with Er decreases the surface roughness of the films which increases transmittance compared to the undoped case [22, 23]. Also, the absorption edge of the doped samples is red-shifted to 405 nm. The average transmittance values of all the doped ZnO films are above 85% above 400 nm.

3.2 Study of electrical transport properties of ZnO:Er thin films

The effects of doping concentration on the electrical properties of the films are measured by Van der Pauw Hall measurements technique [24–26]. Figure 6 shows the variation of carrier concentration, mobility and resistivity of Er doped ZnO films in the range of doping range 0 – 5% at room temperature.

As can be seen from Fig. 6, with Er concentration increasing from 0 to 4%, the resistivity of the films decreases from 8.43 to 2.96 Ω cm, and then slightly increases to 3.14 for 5% Er. The point and surface defects, different scattering centers (impurity scattering and lattice scattering) and the free carrier concentration play a crucial role in the resistivity of the films.

The carrier concentration initially increases rapidly up to 4% Er concentration, thereafter decreases slowly for 5% Er. The increase in carrier concentration may be due to the incorporation of Er ions in interstitial positions or replacement of Er⁺³ ions at Zn⁺² cation sites [27]. The decrease of the carrier concentration at 5% Er is because of the increase in grain boundary defects that act as traps for free carriers.

It is further seen from Fig. 6 that the Hall mobility of the films decreases rapidly from $5.55 \times 10^{-1} \text{ cm}^2 \text{ V}^{-1} \text{ s}^{-1}$

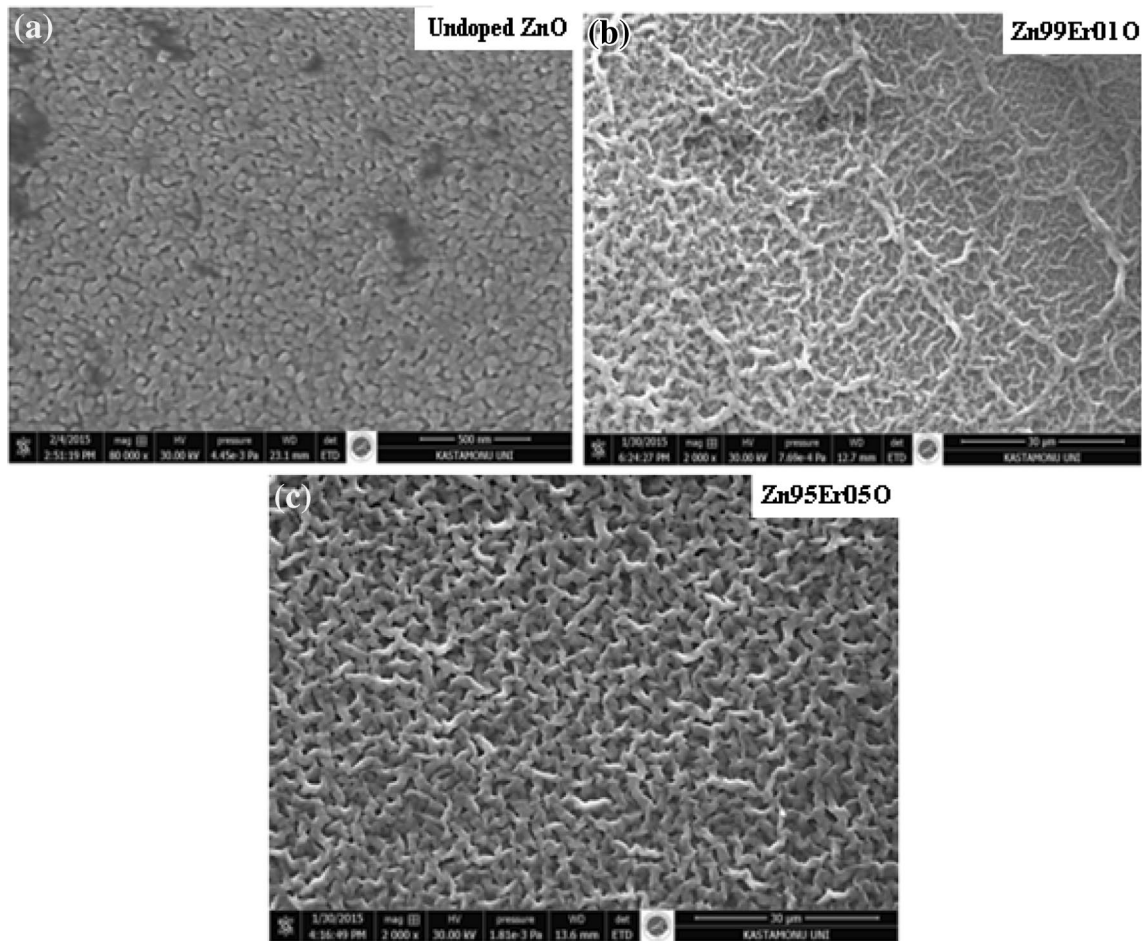


Fig. 3 SEM images of **a** undoped, **b** Zn99Er01O and **c** Zn95Er05O ZnO samples

for undoped ZnO to $2.06 \times 10^{-1} \text{ cm}^2\text{V}^{-1}\text{s}^{-1}$ for 2% Er content, and then increases to 3.69×10^{-1} for 3% Er. For higher Er concentrations, the Hall mobility saturates to $3.7 \times 10^{-1} \text{ cm}^2\text{V}^{-1}\text{s}^{-1}$. The first decrease in Hall mobility can be explained by ionized impurity scattering of the conduction electrons due to Er addition. Because the carrier mobility is governed mainly by the scattering of the charge carriers, the ionized impurity scattering is an important mechanism for the degenerate semiconductors in the low temperature region. The variation of Hall mobility with Er doping is in sync with the variation in grain size given in Table 2. The decrease in grain sizes results in an increase of the number of grain boundaries or vice versa. For 3% and higher doping ratios, the increase in carrier concentration and the scattering centers compensate each other resulting in a stable region of resistivity and mobility.

4 Conclusion

We have presented the results of a study on preparation and characterization of rare-earth Er doped ZnO semiconductor thin films, for Er concentrations of 0.01–0.05. Sol-gel technique was used to grow the nano thin-films while XRD, SEM, AFM and Hall effect measurements were used as characterization techniques. The main findings of our investigation can be summarized as follows:

- XRD data of the films indicate that increasing Er doping is detrimental to the crystallinity of ZnO which is deduced from the decrease in the amplitude of the (002) peak of the spectrum (Fig. 2). These observations were, also, reported in our previous study [18].

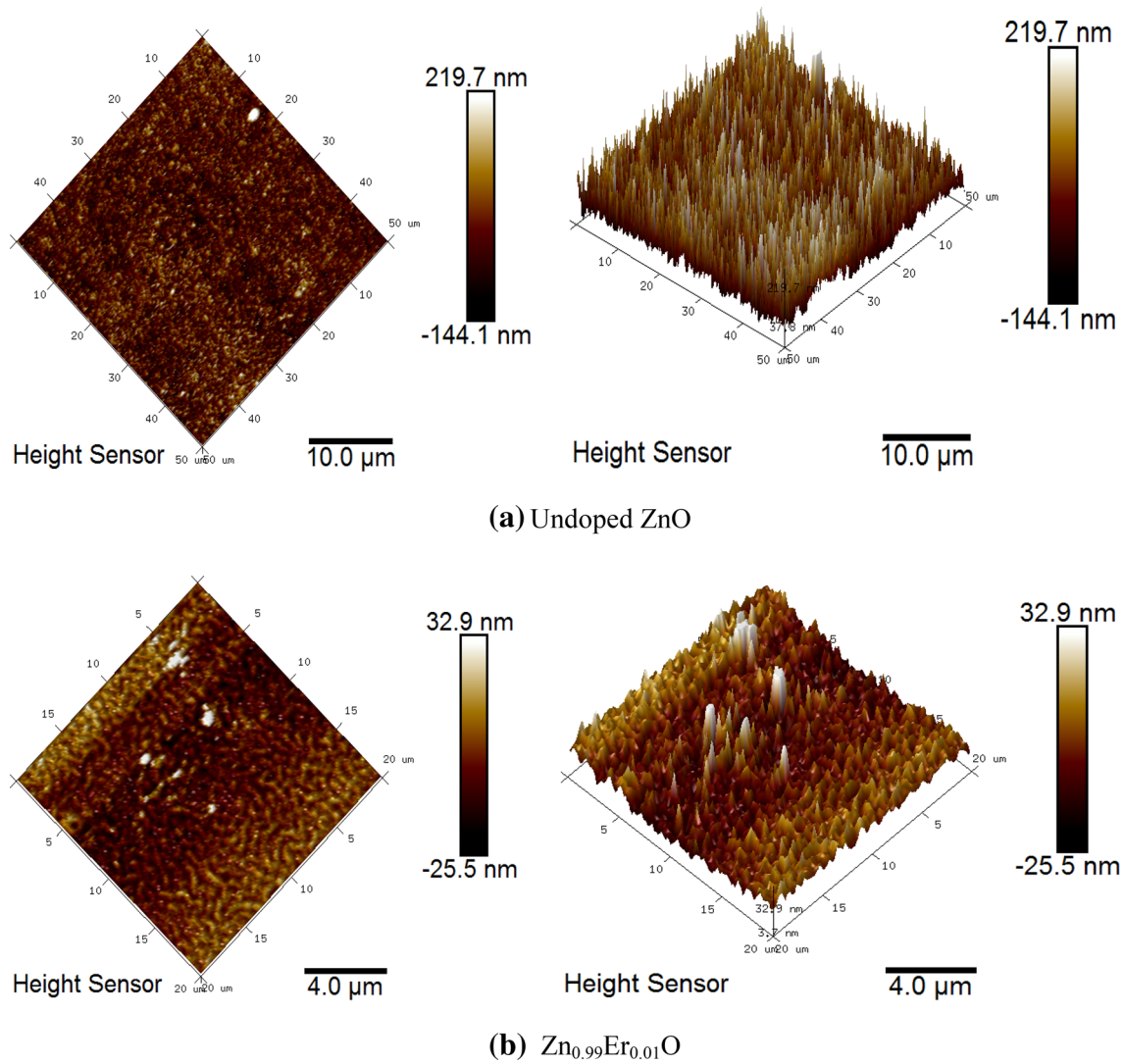
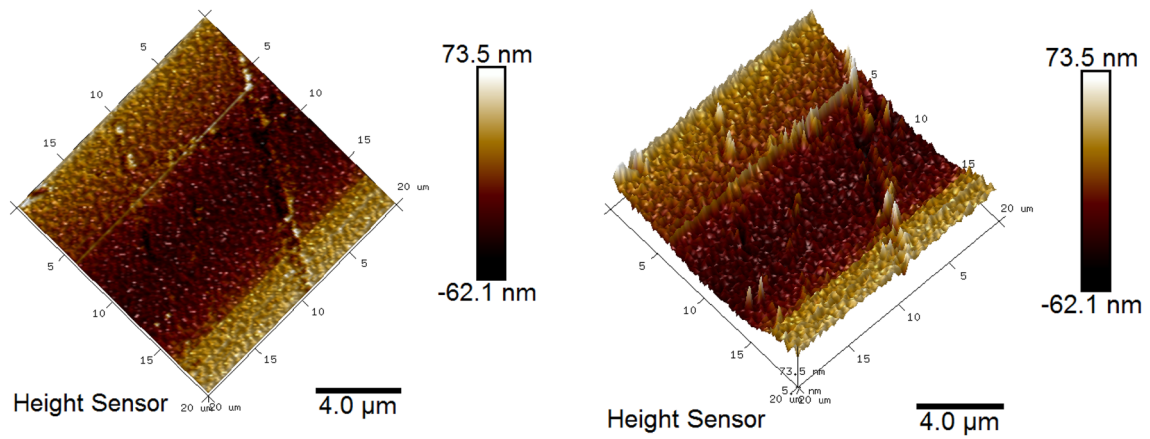


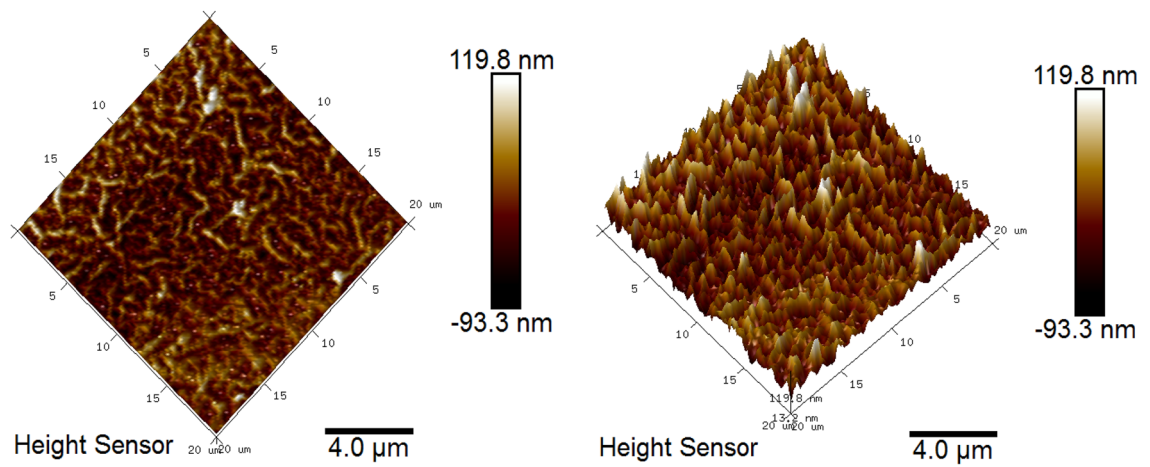
Fig. 4 AFM analyses of all nano thin film materials

- The average grain size decreases with increasing *Er* doping for $Zn_{1-x}Er_xO$ nano thin films. These results are supported by the SEM images as well as XRD data.
- As can be seen from the AFM images, surface roughness is decreased with increasing *Er* doping.
- The resistivity of the films decrease with increasing *Er* concentration from 0 to 4%, and then slightly increase at 5%*Er*.
- Optical transmission in 400–800 nm range is improved by *Er* doping from 81 to 85% for the undoped and doped cases, respectively.

Based on these observations, one can conclude that the rare earth element doping improves important the microstructural, electrical and optical properties of ZnO films.



(c) $\text{Zn}_{0.98}\text{Er}_{0.02}\text{O}$



(d) $\text{Zn}_{0.97}\text{Er}_{0.03}\text{O}$

Fig. 4 (continued)

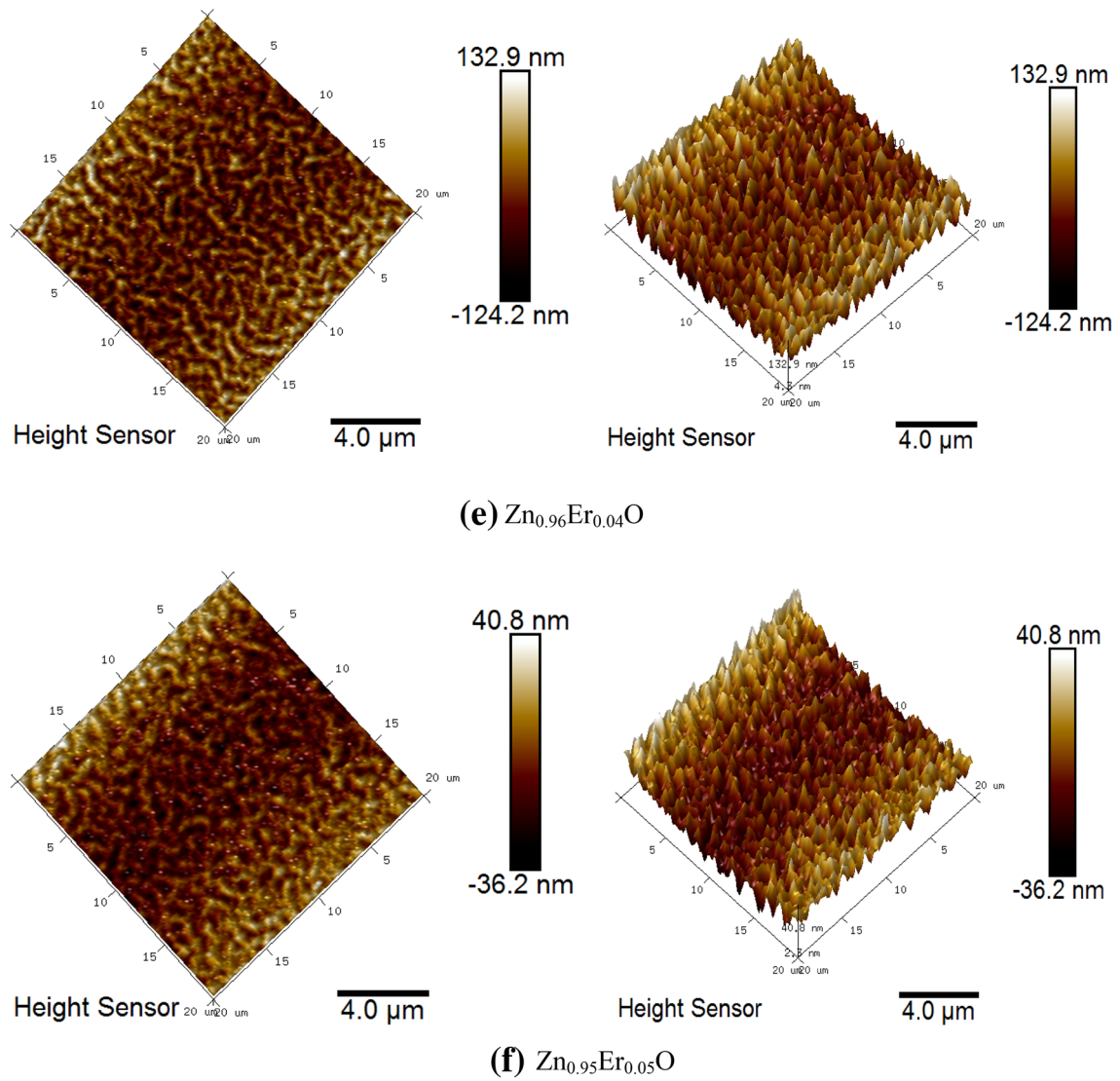
**Fig. 4** (continued)

Fig. 5 Optical transmittance spectra of all ZnO thin films

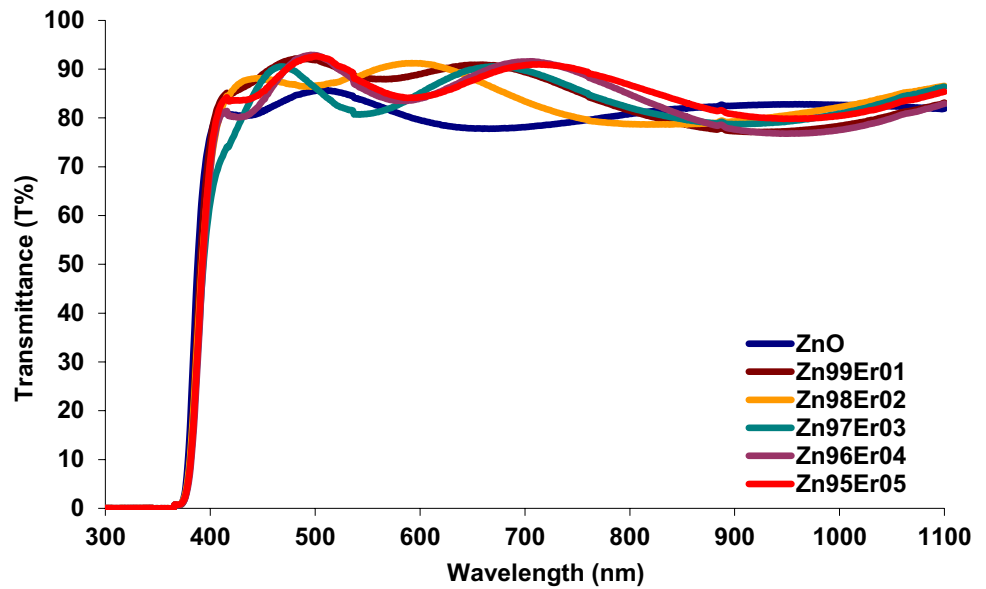
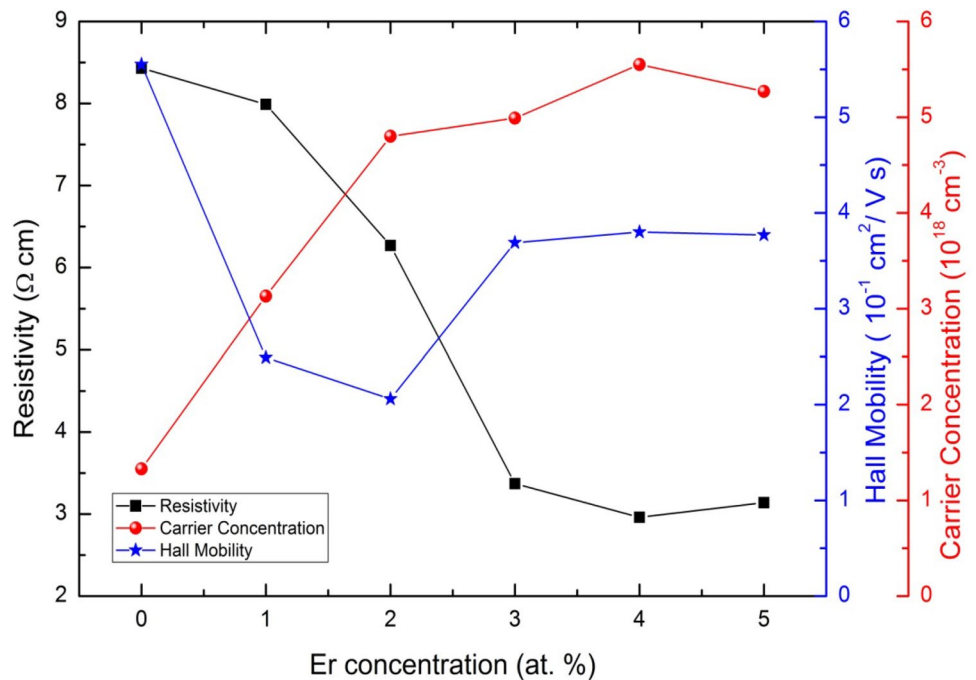


Fig. 6 Dependence of electrical resistivity, carrier concentration and Hall mobility on the Er content



Acknowledgements The authors would like to thank the Kastamonu University Scientific Research Projects Coordination Department under the Grant No. KUBAP-03/2013-41, Grant No. KUBAP-05/2015-12 and the Scientific and Technological Research Council of Turkey (TUBITAK) Project No. 114F259 for the supports.

References

1. Z.K. Heiba, L. Arda, Structural properties of Zn_{1-x}Mg_xO nanomaterials prepared by sol-gel method. *Cryst. Res. Technol.* **44**, 845–850 (2009)
2. S. Zhao, P. Li, Y. Wei, Effects of Ni doping on the luminescent and magnetic behaviors of ZnO nanocrystals. *Powder Technol.* **224**, 390–394 (2012)
3. C.C. Vidyasagar, Y.A. Naik, T.G. Venkatesh, R. Viswanatha, Solid-state synthesis and effect of temperature on optical properties of Cu–ZnO, Cu–CdO and CuO nanoparticles. *Powder Technol.* **214**, 337–343 (2011)
4. S. Muthukumar, R. Gopalakrishnan, Structural, optical and photoluminescence studies of heavily Mn-doped ZnO nanoparticles annealed under Ar atmosphere. *J. Mater. Sci.* **23**, 1393–1401 (2012)
5. Z.K. Heiba, L. Arda, M.B. Mohamed, N.Y. Mostafa, N. Dogan, Effect of annealing temperature on structural and magnetic

- properties of $\text{Zn}_{0.94}\text{Co}_{0.05}\text{Cu}_{0.01}\text{O}$. *J. Supercond. Nov. Magn.* **26**, 3487–3493 (2013)
- X.J. Liu, X.Y. Zhu, J.T. Luo, F. Zeng, F. Pan, Grain boundary defects-mediated room temperature ferromagnetism in Co-doped ZnO film. *J. Alloys Compd.* **482**, 224–228 (2009)
 - G. Pei, C. Xia, F. Wu, J. Xu, Absence of room-temperature ferromagnetism in Al-codoped $\text{Zn}_{0.95}\text{Co}_{0.05}\text{O}$ nanoparticles. *J. Alloys Compd.* **467**, 539–542 (2009)
 - R. Vettumperumal, S. Kalyanaraman, R. Thangavel, Optical constants and near infrared emission of Er doped ZnO sol-gel nano thin films. *J. Lumin.* **158**, 493–500 (2015)
 - W. DeYi, Z. Jian, L. GuiZhen, Effect of Li-doped concentration on the structure, optical and electrical properties of p-type ZnO thin films prepared by sol-gel method. *J. Alloys Compd.* **481**, 802–805 (2009)
 - D.K. Takci, E.S. Tuzemen, K. Kara, S. Yilmaz, R. Esen, O. Baglayan, Influence of Al concentration on structural and optical properties of Al-doped ZnO nano thin films. *J. Mater. Sci.* **25**, 2078–2085 (2014)
 - M. Caglar, Y. Caglar, S. Aksoy, S. Ilcan, Temperature dependence of the optical band gap and electrical conductivity of sol-gel derived undoped and Li-doped ZnO films. *Appl. Surface Sci.* **256**, 4966–4971 (2010)
 - Z. Fan, J.G. Lu, Zinc oxide nanostructures: synthesis and properties. *J. Nanosci. Nanotechnol.* **5**, 1561–1573 (2005)
 - N. Kılınç, L. Arda, S. Öztürk, Z.Z. Öztürk, Structure and electrical properties of Mg-doped ZnO nanoparticles. *Cryst. Res. Technol.* **4**, 529–538 (2010)
 - M. Girtan, M. Socol, B. Pattier, M. Sylla, A. Stanculescu, On the structural, morphological, optical and electrical properties of sol-gel deposited ZnO: in films. *Thin Solid Films* **519**, 573–577 (2010)
 - M. Tosun, S. Ataoglu, L. Arda, O. Ozturk, E. Asikuzun, D. Akcan, O. Cakiroglu, Structural and mechanical properties of ZnMgO nanoparticles. *Mater. Sci. Eng. A* **590**, 416–422 (2014)
 - L. Arda, O. Ozturk, E. Asikuzun, S. Ataoglu, Structural and mechanical properties of transition metals doped ZnMgO nanoparticles. *Powder Technol.* **235**, 479–484 (2013)
 - E.J. Luna-Arredondo, A. Maldonado, R. Asomoza, D.R. Acosta, M.A. Mele'ndez-Lira, M. de la, L. Olvera, Indium-doped ZnO thin films deposited by the sol-gel technique. *Thin Solid Films* **490**, 132–136 (2005)
 - J.G. Lu, Z.Z. Ye, Y.J. Zeng, L.P. Zhu, L. Wang, J. Yuan, Q.L. Liang, Structural, optical, and electrical properties of (Zn, Al) O films over a wide range of compositions. *J. Appl. Phys.* **100**, 073714 (2006)
 - S.D. Senol, O. Ozturk, C. Terzioğlu, Effect of boron doping on the structural, optical and electrical properties of ZnO nanoparticles produced by the hydrothermal method. *Ceram. Int.* **41**, 11194–11201 (2015)
 - K. Necmettin, O. Sadullah, A. Lutfi, A. Ahmet, Z.O. Zafer, Structural, electrical, transport and NO_2 sensing properties of Y-doped ZnO nano thin films. *J. Alloys Compd.* **536**, 138–144 (2012)
 - E. Asikuzun, A. Donmez, L. Arda, O. Cakiroglu, O. Ozturk, D. Akcan, C. Terzioğlu, Structural and mechanical properties of (Co/Mg) co-doped nano ZnO. *Ceram. Int.* **41**, 6326–6334 (2015)
 - E. Asikuzun, O. Ozturk, L. Arda, A.T. Tasci, F. Kartal, C. Terzioğlu, High-quality c-axis oriented non-vacuum Er doped ZnO thin films. *Ceram. Int.* **2**, 8085–8091 (2016)
 - C.Y. Tsay, K.S. Fan, Y.W. Wang, C.J. Chang, Y.K. Tseng, C.K. Lin, Transparent semiconductor zinc oxide nano thin films deposited on glass substrates by sol-gel process. *Ceram. Int.* **36**, 1791–1795 (2010)
 - S.D. Senol, A. Senol, O. Ozturk, M. Erdem, Effect of annealing time on the structural, optical and electrical characteristics of DC sputtered ITO nano thin films. *J. Mater. Sci.* **25**, 4992–4999 (2014)
 - C.Y. Tsay, W.T. Hsu, Sol-gel derived undoped and boron-doped ZnO semiconductor thin films: preparation and characterization. *Ceram. Int.* **39**, 7425–7432 (2013)
 - L.J. Van der Pauw, A method of measuring the resistivity and Hall coefficient on lamellae of arbitrary shape. *Philips Tech. Rev.* **20**, 220–224 (1958)
 - I. Winer, G.E. Shter, M. Mann-Lahav, G.S. Grader, Effect of solvents and stabilizers on sol-gel deposition of Ga-doped zinc oxide TCO films. *J. Mater. Res.* **26**, 1309–1315 (2011)